

# Regularized universal topological local markers for Dirac systems

Yulin Qin,<sup>1,2</sup> Chang-An Li,<sup>3,4</sup> and Jian Li<sup>2</sup>

<sup>1</sup>*Department of Physics, Fudan University, Shanghai 200433, China*

<sup>2</sup>*Department of Physics, School of Science, Westlake University, Hangzhou 310024, Zhejiang, China*

<sup>3</sup>*Institute for Theoretical Physics and Astrophysics,*

*University of Würzburg, 97074 Würzburg, Germany*

<sup>4</sup>*Würzburg-Dresden Cluster of Excellence ct.qmat, Germany*

(Dated: January 1, 2026)

Local markers provide an efficient and powerful characterization of topological features of many systems, especially when the translation symmetry is broken. Recently, a universal topological local marker applicable in different symmetry classes of topological systems is proposed. However, it suffers from irregular behaviors at the boundary and its connection to other topological indexes remains elusive. In this work, we construct regularized universal topological local markers that apply to Dirac systems by utilizing position operators that are compatible with periodic boundary conditions. The regularized local markers eliminate the obstructive boundary irregularities successfully, and give rise to the desired global topological invariants such as the Chern number consistently when integrated over all the lattice sites. Furthermore, the regularized form allows us to establish an explicit connection between the local markers and some other known topological indices in two dimensions. For instance, it turns out to be equivalent to the Bott index in classes A, D, and C, and equivalent to the spin Chern number in classes DIII and AII. We further examine the utility and stability of this new marker in disordered scenarios. We find that its variance shows peaks at the phase boundaries, which promotes it as a useful indicator for detecting disorder-induced topological phase transitions.

## I. INTRODUCTION

Topological invariants serve as the most essential and fundamental characterizations of topological phases of matter in different symmetry classes [1–19]. In general, topological invariants are defined based on band theory and can be obtained by homotopy maps from the Brillouin zone (BZ) to a target manifold, which relies on the translation symmetry of the interested systems. Topological properties can survive when the translation symmetry is broken, for instance, in the disordered system, while the calculation of topological invariants in real space is not straightforward. Substantial progresses have been made in the real space representation of the topological invariants. For example, the real space representation of the Chern number can be derived from the perspective of non-commutative geometry [20–26] and from the Bott index formula [27–30]. There are also the real space representation of the winding number for chiral symmetric systems [31, 32] and the real space local markers [33–42]. A natural question arises: can these invariants be represented uniformly for any symmetry class in any spatial dimension?

Recently, a topological invariant in momentum space called the wrapping number has been proposed along this direction [43]. This progress further sheds light on its real-space representations. Subsequently, universal topological local markers have been further constructed [44]. However, there are two main issues with these universal topological local markers. First, they do not respect translation symmetry even in clean systems. These local markers are invalid near the boundaries of the lattice system, showing boundary irregularities, since the

real space position operators employed therein are not periodic. Second, the desired global properties are not encoded in these local markers. In other words, averaging these local markers over all sites does not yield the desired global topological invariant, making them inapplicable when considering the influence of disorder on global properties.

In this work, we present a regularized universal topological local marker that overcomes the two difficulties aforementioned and exhibits more rich physical consequences. Based on the degree of the orientation vector that describes Dirac systems, we construct a new universal topological local marker by introducing position operators that are consistent with periodic boundary conditions. It thus shows translation symmetry globally and avoids the undesired boundary irregularities. The corresponding topological invariant, such as the Chern number, can further be obtained by summing the local markers over all lattice sites. Remarkably, based on the new formula, we can address the direct connections between the universal topological local markers and other topological invariants in two dimensions (2D). We find that the new formula is equivalent to the Bott index for symmetry classes A, D, and C, and to spin Chern number for classes DIII and AII. Besides, since the global properties are actually encoded in the new local marker, its local fluctuation provides essential information of the disordered topological systems. Its variance peaks at the phase boundaries, which can be used as an indicator for disorder-induced topological phase transitions.

The rest of the paper is organized as follows. In Sec. II, we review the definition of the wrapping number for topological insulators and superconductors described by

the Dirac model, and then present our regularized universal topological local markers. In Sec. III, we demonstrate the connection between the new formula and the Bott index formula in 2D. In Sec. IV, we provide numerical results by applying the new formula to lattice systems so as to consider the influence of disorder and study the fluctuations of these local markers. Finally, we present our conclusions in Sec. V.

## II. REGULARIZED UNIVERSAL TOPOLOGICAL LOCAL MARKERS FROM THE WRAPPING NUMBER

The Dirac model describing topological insulators and superconductors in  $D$  dimensions can be expressed in momentum space as [2, 5, 8]

$$H_0(\mathbf{k}) = \mathbf{d}(\mathbf{k}) \cdot \boldsymbol{\Gamma} = d(\mathbf{k}) \mathbf{n}(\mathbf{k}) \cdot \boldsymbol{\Gamma}, \quad (1)$$

where  $\boldsymbol{\Gamma} = (\Gamma_0, \Gamma_1, \dots, \Gamma_D)$  is a vector composed of a subset of the Dirac matrices  $\{\Gamma_0, \Gamma_1, \dots, \Gamma_{2s}\}$  that satisfy the anti-commutation relations  $\{\Gamma_i, \Gamma_j\} = 2\delta_{i,j}$  and  $s = \lfloor \frac{D+1}{2} \rfloor$  or  $s = \lfloor \frac{D+3}{2} \rfloor$ , depending on the symmetry class [5];  $\mathbf{d}(\mathbf{k}) = (d_0(\mathbf{k}), d_1(\mathbf{k}), \dots, d_D(\mathbf{k}))$  is a vector in  $D+1$  dimensions that characterizes the momentum dependence of the model and  $d(\mathbf{k}) = |\mathbf{d}(\mathbf{k})|$ . Importantly,  $\mathbf{n}(\mathbf{k}) = \mathbf{d}(\mathbf{k})/|\mathbf{d}(\mathbf{k})|$  is the orientation vector of  $\mathbf{d}(\mathbf{k})$ , which is a map from the torus  $T^D$  to the sphere  $S^D$ . According to the Hopf degree theorem [45], the homotopy classification of such maps is determined by the wrapping number or equivalently the degree of the map  $\mathbf{n}(\mathbf{k})$ , which is defined as

$$\deg[\mathbf{n}] = \int_{\text{BZ}} \frac{d^D \mathbf{k}}{V_D} \epsilon_{i_0 \dots i_D} n^{i_0} \partial_{k_1} n^{i_1} \partial_{k_2} n^{i_2} \dots \partial_{k_D} n^{i_D}, \quad (2)$$

where  $V_D$  is the volume of the unite sphere  $S^D$  in  $D$  dimensions. It turns out that this wrapping number captures the topological invariants for various symmetry classes and spatial dimensions for topological insulators and superconductors, thus serving as a unified topological invariant [43]. Considering the flattened Hamiltonian  $H(\mathbf{k}) = \mathbf{n}(\mathbf{k}) \cdot \boldsymbol{\Gamma}$ , the wrapping number can be further expressed as [44]

$$\deg[\mathbf{n}] = \int_{\text{BZ}} \frac{d^D \mathbf{k}}{2^s c V_D} \text{Tr}[W H \partial_{k_1} H \partial_{k_2} H \dots \partial_{k_D} H], \quad (3)$$

where  $2^s c = \text{Tr}[\Gamma_{D+1} \Gamma_{D+2} \dots \Gamma_{2s} \Gamma_0 \Gamma_1 \dots \Gamma_D]$  and  $c \in \{1, i, -i, -1\}$  depending on the order of these matrices and the value of  $s$ . The matrix  $W$  is the product of remaining Dirac matrices defined as  $W \equiv \Gamma_{D+1} \Gamma_{D+2} \dots \Gamma_{2s}$ .

In the following, we demonstrate how to construct a well-defined topological local marker from this wrapping number. Without loss of generality, we consider a quadratic Hamiltonian for a free fermionic system with

translation symmetry, which can be expressed in either the real space or the momentum space as

$$H = \sum_{\mathbf{r}, \mathbf{r}'} H_{\mathbf{r}, \mathbf{r}'} |\mathbf{r}\rangle \langle \mathbf{r}'| = \sum_{\mathbf{k}} H_{\mathbf{k}} |\mathbf{k}\rangle \langle \mathbf{k}|, \quad (4)$$

where we have absorbed all inner degree of freedom in the position basis  $|\mathbf{r}\rangle$  or the momentum basis  $|\mathbf{k}\rangle$  for brevity. Defining the momentum translation operator along the  $i$ -th direction (i.e., the real space position operator) as

$$\hat{X}_i = \sum_{\mathbf{k}} |\mathbf{k} - \delta \mathbf{k}_i\rangle \langle \mathbf{k}| = \sum_{\mathbf{r}} e^{-i\delta \mathbf{k}_i \cdot \mathbf{r}} |\mathbf{r}\rangle \langle \mathbf{r}|, \quad (5)$$

with  $\delta \mathbf{k}_i = \frac{2\pi}{L_i} \mathbf{e}_i$ , where  $L_i$  is the total number of unit cells along the  $i$ -th direction and  $\mathbf{e}_i$  is the unit vector. We then obtain a useful relation

$$\hat{X}_i H \hat{X}_i^\dagger = \sum_{\mathbf{k}} H_{\mathbf{k} + \delta \mathbf{k}_i} |\mathbf{k}\rangle \langle \mathbf{k}|, \quad (6)$$

which helps us to transfer the intergral in the wrapping number approximately as

$$\begin{aligned} & \int d^D \mathbf{k} W H \partial_{k_1} H \partial_{k_2} H \dots \partial_{k_D} H \\ & \sim \frac{1}{2^D} \sum_{\mathbf{k}} W H_{\mathbf{k}} \prod_{i=1}^D (H_{\mathbf{k} + \delta \mathbf{k}_i} - H_{\mathbf{k} - \delta \mathbf{k}_i}) \\ & = \frac{1}{2^D} \text{Tr} \left[ W H \prod_{i=1}^D (X_i H X_i^\dagger - X_i^\dagger H X_i) \right]. \end{aligned} \quad (7)$$

Note that we have written all the operators in real space, using  $W$  to represent  $I_N \otimes W$  for brevity where  $I_N$  is the  $N$  dimensional identity matrix. Consequently, the wraping number is writen as

$$\deg[\mathbf{n}] = \frac{1}{2^s c V_D 2^D} \text{Tr} \left[ W H \prod_{i=1}^D (X_i H X_i^\dagger - X_i^\dagger H X_i) \right], \quad (8)$$

where  $X_i = e^{-i\frac{2\pi}{L_i} \hat{x}_i}$  is real space representation of the momentum translation operator along the  $i$ -th direction.

Finally, we arrive at the following universal topological operator

$$\hat{C} = \frac{N}{2^s c V_D 2^D} W H \prod_{i=1}^D (X_i H X_i^\dagger - X_i^\dagger H X_i), \quad (9)$$

where the factor  $N$  is defined as  $N = \prod_{i=1}^D L_i$  being the total number of the unit cells. We denote its local value

$$C(\mathbf{r}) = \sum_{\ell} \langle \mathbf{r}, \ell | \hat{C} | \mathbf{r}, \ell \rangle \quad (10)$$

as a universal topological local marker, where  $\ell$  indicates the inner degrees of freedom at site  $\mathbf{r}$ . From this definition, the wrapping number can be expressed as

$$\deg[\mathbf{n}] = \frac{\text{Tr}[\hat{C}]}{N} = \bar{C}. \quad (11)$$

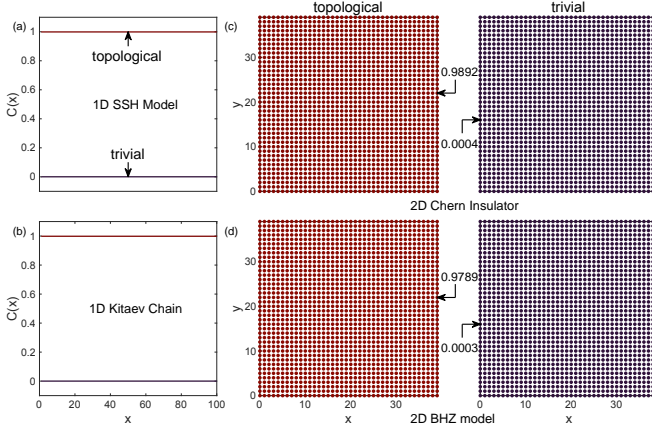


FIG. 1. Regularized universal topological local markers for various models: (a) for 1D SSH model; (b) for 1D Kitaev Chain; (c) for 2D Chern Insulator; and (d) for 2D BHZ model. In (a) and (b), we use a lattice of 100 unite cells; in (c) and (d), we use a lattice of  $40 \times 40$  unite cells. The parameters used in each model are detailed in Appendix A. In all cases, the local markers distribute uniformly and converge to the expected topological invariant representing the corresponding phase.

Equations (9,10,11) present the main results of our work.

This universal topological local marker  $C(\mathbf{r})$  demonstrates several remarkable properties. First, it is fully compatible with periodic boundary conditions. The position operator  $X_i$  in Eq. (9) is well-defined for lattice Hamiltonian. It maintains translation symmetry for clean systems. If we translate the whole system along  $i$ -th direction, a global phase is introduced in operator  $X_i$ . This global phase will be canceled by  $X_i^\dagger$ , thus the whole expression remains invariant. Therefore, the local markers  $C(\mathbf{r})$  are uniformly distributed at site  $\mathbf{r}$ , even when  $\mathbf{r}$  is close to the boundaries. This means that  $C(\mathbf{r})$  does not suffer from boundary irregularities for finite-size lattices as seen in [44]. Explicitly, we apply our formula to prototypical topological models, i.e., the Su-Schrieffer-Heeger (SSH) model [13] and Kitaev chain model [14] in 1D, and Chern insulator and Benervig-Hughes-Zhang (BHZ) model [19] in 2D. We present the main results in Fig. 1 and leave the details of these models in Appendix A. It is found that the topological local markers are uniformly quantized at  $C(\mathbf{r}) = 1$  for topological non-trivial phases and  $C(\mathbf{r}) = 0$  for trivial phases, which provide proper characterization for the corresponding models. Second, the global topological invariant is entirely encoded in these local markers. This feature, being more relevant when disorder is taken into account, enables us to derive the precise global topological invariant by averaging the local markers over all the lattice sites. As such, the universal topological local marker  $C(\mathbf{r})$  permits an explicit connection with other real space representation of topological invariants such as the Bott index formula for 2D system, as shown in the following Sec. III. Third, the fluctuations of these local markers could serve as an indicator for topological phase transitions induced

by disorder whereas the average value of these local markers represents the global topological invariant. We will elaborate this point in details in Sec. IV.

### III. CONNECTION WITH THE BOTT INDEX FORMULA IN TWO DIMENSIONS

The Bott index formula is a powerful tool to calculate the Chern number [28] and the spin Chern number [46]. In this section, we explicitly demonstrate the connection between our topological local markers and the Bott index in 2D.

#### A. Symmetry classes A, D, and C

For symmetry class A, D and C in 2D, we consider the minima Dirac model whose flattened Hamiltonian in momentum space can be expressed as  $H(\mathbf{k}) = \mathbf{n}(\mathbf{k}) \cdot \boldsymbol{\sigma}$ , where  $\boldsymbol{\sigma} = (\sigma_x, \sigma_y, \sigma_z)$  is the Pauli matrix vector. In these cases,  $W$  is the identity matrix,  $2^s c = \text{tr}[\sigma_x \sigma_y \sigma_z] = 2i$ . The corresponding wrapping number is

$$\begin{aligned} \text{deg}[\mathbf{n}] &= \frac{1}{8\pi i} \text{Tr}[H(XPX^\dagger - X^\dagger PX)(YPY^\dagger - Y^\dagger PY)] \\ &= \frac{1}{2\pi i} \text{Tr}\left[\frac{1}{2}(QXPYQX^\dagger PY^\dagger - QXPY^\dagger QX^\dagger PY)\right. \\ &\quad \left.- \frac{1}{2}(PXPYPX^\dagger PY^\dagger - PXPY^\dagger PX^\dagger PY)\right], \end{aligned} \quad (12)$$

where we have used the fact that  $H = Q - P = 1 - 2P$  with  $P(Q)$  being the projection operator to the occupied(un-occupied) states,  $X, Y, X^\dagger, Y^\dagger$  are position operators commuting with each other, as well as the cyclical invariance under trace operation.

It is well-known [28, 29, 47] that the norms  $\| [X, P] \|$  and  $\| [Y, P] \|$  are of order  $O(1/L)$  for a local, bounded Hamiltonian with a finite gap, therefore

$$\begin{aligned} &\text{Tr}\left[\frac{1}{2}(QXPYQX^\dagger PY^\dagger - QXPY^\dagger QX^\dagger PY)\right] \\ &= \text{Tr}\left[\frac{1}{2}([X, P]P[P, Y][X^\dagger, P]P[P, Y^\dagger]\right. \\ &\quad \left.- [X, P]P[P, Y^\dagger][X^\dagger, P]P[P, Y])\right] \\ &\sim O\left(\frac{1}{L_x L_y}\right) \xrightarrow{L_x, L_y \rightarrow \infty} 0. \end{aligned} \quad (13)$$

Here, we have used  $QAP = (1 - P)AP = [A, P]P$  and  $PAQ = PA(1 - P) = P[P, A]$  for arbitrary  $A$ . It is worth noting that in the presence of certain additional symmetry, for instance the particle-hole symmetry  $S$  which relates  $P$  and  $Q$  by  $SPS^{-1} = Q$  and  $SQS^{-1} = P$ , Eq. (13) is valid regardless of the lattice size. To show this, notice that  $S$  is anti-unitary operator, thus we have

$$\text{Tr}[QXPYQX^\dagger PY^\dagger]$$

$$\begin{aligned}
&= \text{Tr}[SQXPYQX^\dagger PY^\dagger S^{-1}]^* \\
&= \text{Tr}[PX^\dagger QY^\dagger PXQY]^* \\
&= \text{Tr}[(PX^\dagger QY^\dagger PXQY)^\dagger] \\
&= \text{Tr}[QXPY^\dagger QX^\dagger PY]. \tag{14}
\end{aligned}$$

In general, we conclude

$$\begin{aligned}
\deg[\mathbf{n}] &= \frac{1}{2\pi i} \text{Tr}[\frac{1}{2}(PXPY^\dagger PX^\dagger PY - PXPYPX^\dagger PY^\dagger)] \\
&= \frac{1}{2\pi i} \text{Tr}[\frac{1}{2}(U_Y U_X U_Y^\dagger U_X^\dagger - U_X U_Y U_X^\dagger U_Y^\dagger)], \tag{15}
\end{aligned}$$

where we have defined non-singular matrices  $U_X = \langle \psi_{\text{occ}} | X | \psi_{\text{occ}} \rangle$  and  $U_Y = \langle \psi_{\text{occ}} | Y | \psi_{\text{occ}} \rangle$  with  $|\psi_{\text{occ}}\rangle = (|\psi_{1,\text{occ}}\rangle, |\psi_{2,\text{occ}}\rangle, \dots)$  being the matrix composed of all eigenvectors for the occupied states. Further denoting  $U = U_Y U_X U_Y^\dagger U_X^\dagger$ , we obtain [29, 48]

$$\begin{aligned}
\deg[\mathbf{n}] &= \frac{1}{2\pi i} \text{Tr}[\frac{1}{2}(U - U^\dagger)] = \frac{1}{2\pi} \text{Im}(\text{Tr}[U]) \\
&= \frac{1}{2\pi} \text{Im}(\text{Tr}[\log(U)]) + O(\frac{1}{L_x L_y}) \\
&= \frac{1}{2\pi} \text{Im}(\text{Tr}[\log(U)]) \quad (L_x, L_y \rightarrow \infty). \tag{16}
\end{aligned}$$

The right side of this equation is nothing but the Bott index formula in 2D. Finally, we arrive at the important relation

$$\bar{C} = \frac{1}{2\pi} \text{Im}(\text{Tr}[\log(U)]), \tag{17}$$

which connects our topological local markers to the Bott index.

In order to demonstrate this connection more transparently, we consider an explicit D class Dirac Hamiltonian given in momentum space by [8]

$$\begin{aligned}
H_D(\mathbf{k}) &= (2t \cos k_x + 2t \cos k_y - \mu) \sigma_z \\
&+ 2\Delta \sin k_x \sigma_x + 2\Delta \sin k_y \sigma_y, \tag{18}
\end{aligned}$$

where the particle-hole operator can be expressed as  $\sigma_x K$  with  $K$  being the complex conjugation and the product of remaining Dirac matrices is  $W = \sigma_0$ . Here,  $t$  is the hopping integral,  $\mu$  is the chemical potential, and  $\Delta$  is the pairing amplitude. We employ a lattice of  $40 \times 40$  unite cells for numerical simulation and the results are presented in Fig. 2. It is clear that our new topological local markers are consistent with the Bott index formula [28], capturing the topological phases and phase transitions successfully. The slight deviation of our results from the Bott index could arise from finite size effect. Therefore, the averaged topological local markers provide a reliable approximation to the Bott index formula.

## B. Symmetry class DIII and AII

For symmetry classes DIII and AII, we employ the strategy of dimensional reduction to show the connections directly [5]. In 2D, three Dirac matrices  $\{\gamma_1, \gamma_2, \gamma_3\}$

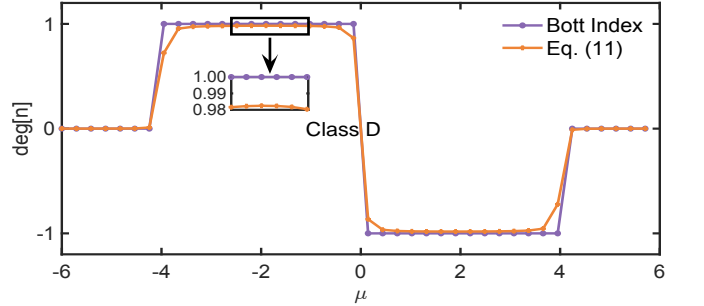


FIG. 2. Comparison for topological local markers and the Bott index formula to verify Eq. 17. We use the two-dimensional system of symmetry classes D in this numerical simulation. The parameters are  $t = -1, \Delta = 0.5$ . The inset provides a close-up for partial detail.

out of the five  $\{\gamma_1, \gamma_2, \gamma_3, \gamma_4, \gamma_5\}$  are employed to construct the minimal Dirac Hamiltonian as

$$H_{\text{DIII(AII)}}(\mathbf{k}) = n_1(\mathbf{k})\gamma_1 + n_2(\mathbf{k})\gamma_2 + n_3(\mathbf{k})\gamma_3. \tag{19}$$

In this case,  $W$  is the product of two Dirac matrices that commutes with  $H$ . Thus we can further define  $W = \gamma_4\gamma_5 \equiv iS_z$ , where  $S_z$  is Hermitian and traceless. The  $S_z$  squares to identity, and we call it the generalized spin polarization operator. Since  $2^s c = \text{Tr}[\gamma_4\gamma_5\gamma_1\gamma_2\gamma_3] = (2i)^2$  in this case, and note that  $I_N \otimes W$  also commutes with  $X, Y, X^\dagger$ , and  $Y^\dagger$ , we arrive at

$$\begin{aligned}
\deg[\mathbf{n}] &= \frac{1}{2i} \frac{1}{2\pi i} \text{Tr}[\frac{1}{2}W(PXPY^\dagger PX^\dagger PY \\
&\quad - PXPYPX^\dagger PY^\dagger)] \\
&= \frac{1}{2} \frac{1}{2\pi i} \text{Tr}[\frac{1}{2}S_z(PXPY^\dagger PX^\dagger PY \\
&\quad - PXPYPX^\dagger PY^\dagger)], \tag{20}
\end{aligned}$$

where we have shortened  $I_N \otimes W(I_N \otimes S_z)$  as  $W(S_z)$  for brevity. On the other hand,  $S_z = S_+ - S_-$ , where  $S_+(S_-)$  is the projection onto the  $+1(-1)$  eigenspace of the operator  $S_z$ . Besides, the eigenvectors for the occupied states can be divided into two sectors  $|\psi_{\text{occ}}\rangle = (|\psi_{\text{occ},+}\rangle, |\psi_{\text{occ},-}\rangle)$  which correspond to eigenvectors of  $S_z$  with  $\pm 1$  eigen-values respectively. Thus

$$\begin{aligned}
&\text{Tr}[S_z PXPY^\dagger PX^\dagger PY] \\
&= \text{Tr}[(S_+ - S_-)PXPY^\dagger PX^\dagger PY] \\
&= \text{Tr}[P_+ X P_+ Y^\dagger P_+ X^\dagger P_+ Y - P_- X P_- Y^\dagger P_- X^\dagger P_- Y] \\
&= \text{Tr}[U_{Y,+} U_{X,+} U_{Y,+}^\dagger U_{X,+}^\dagger - U_{Y,-} U_{X,-} U_{Y,-}^\dagger U_{X,-}^\dagger], \tag{21}
\end{aligned}$$

where we have used the fact that  $S_+ + S_- = I, S_\pm A S_\mp = 0$  for any  $A \in \{P, X, Y, X^\dagger, Y^\dagger\}$  since  $S_z$  commutes with them.  $P_\pm = S_\pm P S_\pm = |\psi_{\text{occ},\pm}\rangle\langle\psi_{\text{occ},\pm}|$  and we have defined non-singular matrices  $U_{X,\pm} = \langle\psi_{\text{occ},\pm}| X | \psi_{\text{occ},\pm}\rangle$  and  $U_{Y,\pm} = \langle\psi_{\text{occ},\pm}| Y | \psi_{\text{occ},\pm}\rangle$ . A similar expression can

be derived for the second term in equation (20). Further denoting  $U_{\pm} = U_{Y,\pm}U_{X,\pm}U_{Y,\pm}^{\dagger}U_{X,\pm}^{\dagger}$ , we obtain

$$\begin{aligned} \text{deg}[\mathbf{n}] &= \frac{1}{2} \frac{1}{2\pi i} \text{Tr} \left[ \frac{1}{2} (U_+ - U_-) - \frac{1}{2} (U_+^{\dagger} - U_-^{\dagger}) \right] \\ &= \frac{1}{2} \frac{1}{2\pi} \text{Im}(\text{Tr}[U_+] - \text{Tr}[U_-]) \\ &= \frac{1}{2} \frac{1}{2\pi} \text{Im}(\text{Tr}[\log(U_+)] - \text{Tr}[\log(U_-)]) + O\left(\frac{1}{L_x L_y}\right) \\ &= \frac{1}{2} (C_+ - C_-) \quad (L_x, L_y \rightarrow \infty), \end{aligned} \quad (22)$$

which equates our topological local marker to the Bott index formula for the spin Chern number with generalized spin operator  $S_z = -iW$  and  $C_{\pm} = \frac{1}{2\pi} \text{Im}(\text{Tr}[\log(U_{\pm})])$  [46, 49].

#### IV. DISORDER EFFECT ON THE UNIVERSAL TOPOLOGICAL LOCAL MARKERS

One most important advantage of topological local markers lies in their applications in disordered systems when the translation symmetry is lost. Due to the remarkable properties mentioned above, our regularized topological local markers not only give rise to the global topological invariants by integrating over all lattice sites, but also provide signatures of topological phase transitions via their local fluctuations in disordered systems. In the following, we demonstrate the direct influence of disorder on topological local markers, taking 1D BDI and D class topological models as concrete examples.

##### A. Class BDI in one dimension

For symmetry class BDI in 1D, we consider the extended SSH model. The disordered Hamiltonian with next-nearest couplings can be expressed as [50]

$$H_1 = \sum_i (t_{0,i} c_{i,A}^{\dagger} c_{i,B} + t_{1,i} c_{i+1,A}^{\dagger} c_{i,B} + t_{2,i} c_{i+2,A}^{\dagger} c_{i,B}) + h.c., \quad (23)$$

where the parameters are set to be  $t_{0,i} = m + \Omega \omega_i$ ,  $t_{1,i} = t_1 + \frac{\Omega}{2} \omega_i$ , and  $t_{2,i} = t_2$ . Here,  $c_{i,A(B)}^{\dagger}$  and  $c_{i,A(B)}$  are the creation and annihilation operators at site  $i$  for A(B) sub-lattice, respectively. The parameter  $\Omega$  represents the disorder strength and  $\omega_i$  is a random number distributes uniformly in  $[-\frac{1}{2}, \frac{1}{2}]$ . For the clean system ( $\Omega = 0$ ), the phase diagram with respect to  $m$  and  $t_2$  by fixing  $t_1 = 1.0$  is illustrated in Fig. 3(a), which is obtained by averaging all the local markers with a lattice size of 500 unite cells. It describes the phase diagram of the extended SSH model properly [50].

The phase diagram with respect to  $m$  and  $\Omega$  is illustrated in Fig. 3(b). For a detailed inspection on the influence of disorder on the global topological invariant and the phase transition induced by disorder, we consider

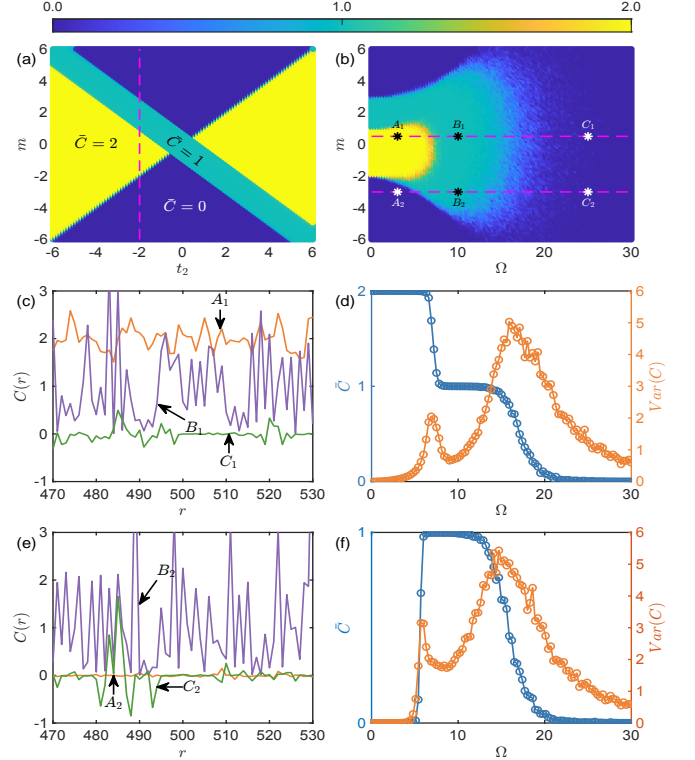


FIG. 3. (a)-(b) Phase diagrams of the extended SSH model: (a) Clean system as a function of  $m$  and  $t_2$  with  $t_1 = 1.0$  and  $\Omega = 0$ , the dashed purple line represent the case  $t_2 = -2.0$ ; (b) Disordered phase diagram as a function of  $m$  and disorder strength  $\Omega$  with  $t_1 = 1.0$  and  $t_2 = -2.0$ . We have averaged over 10 disorder realizations. The two dashed purple lines indicate the cases  $m = 0.5$  and  $m = -3.0$ , respectively.  $A_1, B_1, C_1$  are three points with specific disorder strength on the line  $m = 0.5$ . The corresponding values of local markers at these representative points are presented in (c); Similarly,  $A_2, B_2, C_2$  are three points for the case  $m = -3.0$ . (c) and (e): Local markers  $C(r)$  at specific disorder strengths  $\Omega = 3, 10$ , and 25 for a representative disorder realization (central 60 sites shown), for  $m = 0.5$  and  $m = -3.0$ , respectively. (d) and (f): Global topological invariant  $\bar{C}$  (blue curve, obtained by averaging all the local markers) and corresponding variance  $\text{Var}(C)$  (orange curve) are plotted as functions of the disorder strength  $\Omega$  for  $m = 0.5$  and  $m = -3.0$ , respectively. Each data point is averaged over 100 disorder realizations with system size of 1000 unit cells.

two lines  $m = 0.5$  and  $m = -3$ , indicated in Fig. 3(b). The former one undergoes  $\bar{C} = 2 \rightarrow \bar{C} = 1 \rightarrow \bar{C} = 0$  if we gradually increase the disorder strength  $\Omega$ . While the latter one undergoes  $\bar{C} = 0 \rightarrow \bar{C} = 1 \rightarrow \bar{C} = 0$ , which indicates a topological Anderson phase transition in the extended SSH model [50–52].

In the presence of disorder, the local markers  $C(r)$  are no longer uniformly distributed at each lattice site  $r$ . Figs. 3(c) and 3(e) present the values of local markers for some representative points marked in phase diagram Fig. 3(b), which clearly show the existence of fluctuations of these local markers in disordered systems. To investigate

their local fluctuations, we calculate the variance of these local markers, namely,

$$\text{Var}(C) = \frac{1}{N} \sum_{\mathbf{r}} (C(\mathbf{r}) - \bar{C})^2. \quad (24)$$

Note that the system contains 1000 lattice sites in numerical calculations, and the 100 disorder realizations are averaged. The results are presented in Figs. 3(d) and 3(f) for the two lines  $m = 0.5$  and  $m = -3$ , respectively. For the case  $m = 0.5$ , it is clear that at weak disorder strength, the global topological invariant  $\bar{C}$  remains robust against disorder, maintaining at the value  $\bar{C} = 2$ . The corresponding variance of the local markers increases with the disorder strength. At a critical value of  $\Omega_c^1$ , the variance reaches a local maximum. It then decreases within a small window around  $\Omega_c^1$ . Correspondingly, the global topological invariant gradually drops from  $\bar{C} = 2$  to  $\bar{C} = 1$ , indicating a topological phase transition. Once the system enters the  $\bar{C} = 1$  phase, the variance of the local markers increases until it reaches its next local maximum at  $\Omega_c^2$ , signaling another phase transition from  $\bar{C} = 1$  to  $\bar{C} = 0$  as increasing  $\Omega$ . For the case  $m = -3$ , similar results can be obtained. Thus, these peaks of the variance can serve as indicator of phase transitions induced by disorder.

## B. Class D in one dimension

For symmetry class D in 1D, we consider the Kitaev chain [14] with random onsite chemical potentials. The Hamiltonian is

$$H_2 = \sum_i -\mu_i (c_i^\dagger c_i - \frac{1}{2}) - t \sum_i (c_i^\dagger c_{i+1} + c_{i+1}^\dagger c_i) + \Delta \sum_i (c_{i+1}^\dagger c_i^\dagger + c_i c_{i+1}), \quad (25)$$

where  $\mu_i = \mu - \Omega \omega_i$ ,  $\Omega$  represents the disorder strength and  $\omega_i$  is a random number distributes uniformly in  $[-\frac{1}{2}, \frac{1}{2}]$ . Here,  $t$  and  $\Delta$  are real parameters of this model. In the clean limit ( $\Omega = 0$ ), the system falls into the topological non-trivial phase when  $|\mu| < 2|t|$  and  $\Delta \neq 0$ . The phase diagram with respect to  $\mu$  and  $t$  by fixing  $\Delta = 2.5$  is illustrated in Fig. 4(a). In presence of disorder, the phase diagram with respect to  $\mu$  and  $\Omega$  is illustrated in Fig. 4(b) by fixing  $\Delta = 2.5$  and  $t = 1.0$ . The degree of Dirac Hamiltonian only yields a  $Z$ -valued invariant  $\text{deg}(\mathbf{n})$ , while the Kitaev chain falls into a  $Z_2$  classification. In order to obtain the phase diagram as shown in Figs. 4(a) and 4(b), we have employed  $|\text{deg}(\mathbf{n})| \bmod 2$  as the  $Z_2$  invariant. It can be expressed as the wrapping number in the form  $(-1)^{\text{deg}(\mathbf{n})}$  [43] or equivalently  $\text{deg}(\mathbf{n}) \bmod 2$ , together with the fact that  $-\text{deg}(\mathbf{n}) \equiv \text{deg}(\mathbf{n}) \bmod 2$ . Similarly, we consider two lines  $\mu = -0.5$  and  $\mu = -2.5$ , indicated by dashed lines in Fig. 4(b). The former one undergoes transition  $\bar{C} = 1 \rightarrow \bar{C} = 0$  and the latter one

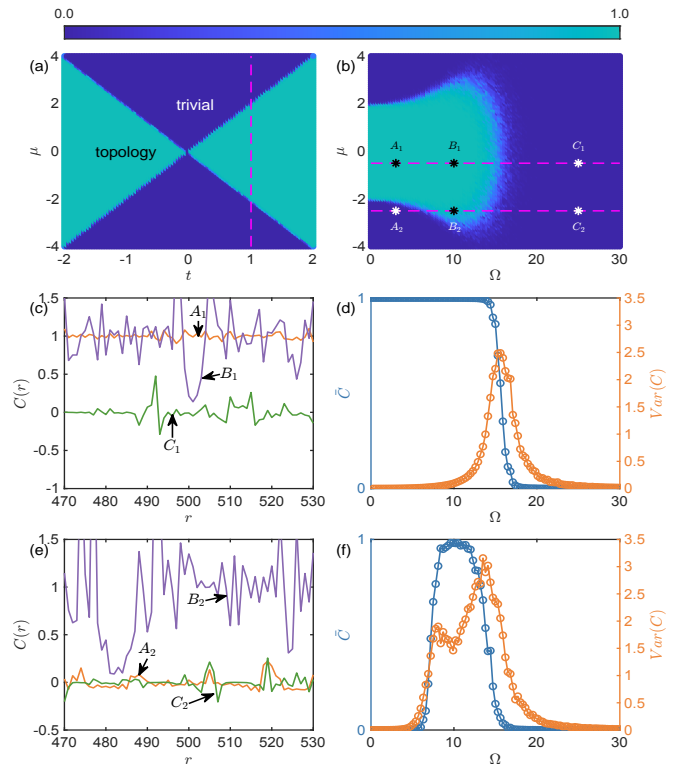


FIG. 4. (a) and (b): Phase diagrams of one dimensional D class Kitaev chain. (a) Clean system as a function of  $\mu$  and  $t$  with  $\Delta = 2.5$  and  $\Omega = 0$ . The dashed purple line represent the case  $t = 1.0$ ; (b) Disordered phase diagram as a function of  $\mu$  and disorder strength  $\Omega$  with  $t = 1.0$  and  $\Delta = 2.5$ . We have averaged 10 disorder realizations. The two dashed purple lines indicate the cases  $\mu = -0.5$  and  $\mu = -2.5$ , respectively.  $A_1, B_1, C_1$  are three points with specific disorder strength on the line  $\mu = -0.5$ , and the corresponding values of local markers at these representative points are presented in (c); Similarly,  $A_2, B_2, C_2$  are three points for the case  $m = -2.5$ . (c) and (e): Local markers  $C(r)$  at specific disorder strengths  $\Omega = 3, 10, 25$  for a representative disorder configuration (central 60 sites shown), for  $\mu = -0.5$  and  $\mu = -2.5$ , respectively. (d) and (f): Global topological invariant  $\bar{C}$  (blue curve, obtained by averaging all local markers) and variance  $\text{Var}(C)$  (orange curve) are plotted as functions of the disorder strength  $\Omega$  for  $\mu = -0.5$  and  $\mu = -2.5$ , respectively. Each data point is averaged over 100 disorder realizations with system size of 1000 unit cells.

undergoes transition  $\bar{C} = 0 \rightarrow \bar{C} = 1 \rightarrow \bar{C} = 0$ , as gradually increasing the disorder strength  $\Omega$ . The behavior of the local markers, the global topological invariant, and the corresponding variance at specific disorder strengths  $\Omega$  are shown in Figs. 4(c)-(f), which is much similar to the case of BDI class discussed before. Thus we can conclude that the local maxima of the variance of the local markers can also serve as indicators of phase transitions induced by disorder in the 1D D class Kitaev chain.

## V. CONCLUSION AND DISCUSSION

In summary, we have introduced a regularized universal topological local marker applicable to any symmetry class and spatial dimension for topological insulators and superconductors described by the Dirac Hamiltonian, constructed from position operators that remain fully compatible with periodic boundary conditions. This formulation successfully removes boundary irregularities and, when summed over all lattice sites, reproduces the expected global topological invariants—such as the Chern number—in a consistent manner. Leveraging this property, we established explicit correspondences between our marker and several established topological indices in two dimensions, demonstrating its equivalence to the Bott index in classes A, D, and C, and to the spin Chern number in classes DIII and AII. Finally, we assessed the robustness of the marker in the presence of disorder and showed that its variance exhibits pronounced peaks at phase boundaries, highlighting its effectiveness as an indicator of disorder-driven topological phase transitions.

We note that the current version of universal topological local markers are applicable only to topological insulators and superconductors that can be described by the Dirac model, at least at low energy. In these cases, the system's flattened Hamiltonian in momentum space can be expressed as  $H(\mathbf{k}) = \mathbf{n}(\mathbf{k}) \cdot \mathbf{\Gamma}$  where the central object in this framework is the degree of  $\mathbf{n}$ , which is a map from  $T^D$  to  $S^D$  for a Dirac Hamiltonian in  $D$  dimensions. Note also that our regularized universal topological local markers can be reduced to the one proposed by Chen [44] in the thermodynamic limit (see Appendix B). There are several questions which call for further investigations in the future. For instance, whether it is possible to uniformly represent all topological invariants for any symmetry class and spatial dimension beyond the Dirac models. One possible strategy is to represent the product of all the unused Dirac matrices—denoted by  $W$  in the main text—by using the local symmetry operators, since only the matrix  $W$  carries the information inherited from the Dirac matrices in Eq. (9). For example, in 2D class A, the matrix  $W$  is simply the identity within the Dirac Hamiltonian system, conveying no additional information about the Dirac matrices. Thus, it may be natural to extend the scope of Eq. (9) in this context to any system belonging to symmetry class A. Prodan et al. have developed a real space formula for the Chern number for any system that closely resembles the formula derived from this strategy [22]. It remains unclear whether this strategy is valid when  $W$  is not the identity or for cases beyond symmetry class A, and this issue requires further investigation.

## VI. ACKNOWLEDGMENTS

This work was supported by the National Natural Science Foundation under Grant No. 92265201 and No. 12574176, and the Innovation Program for Quantum Science and Technology under Project No. 2021ZD0302704. C.A.L. was financially supported by Würzburg-Dresden Cluster of Excellence ct.qmat, EXC2147, project-id 390858490.

## Appendix A: NUMERICAL RESULTS ON THE UNIVERSAL TOPOLOGICAL LOCAL MARKERS

In order to show the effectiveness of the regularized universal topological local markers, we use the following four Dirac models as concrete examples in our numerical simulation since they cover all the four kinds of topological invariants in the ten-fold classification framework [1–8]. We list the Hamiltonian of these models in momentum space to clearly show that they all belong to Dirac system. The corresponding local markers are presented in Fig. 1 in the main text.

### 1. 1D SSH model [13] (The winding number)

$$H_0(k) = (t_0 + t_1 \cos k_x) \sigma_x + t_1 \sin k_x \sigma_y. \quad (\text{A1})$$

The time reversal operator is  $\sigma_0 K$ , particle hole operator is  $\sigma_z K$ , and the Chiral operator is  $\sigma_z$ . The product of all the unused Dirac matrices is  $W = \sigma_z$ . This model Hamiltonian falls into the symmetry class BDI with a Z classification, the associated topological invariant is called the winding number. We fix  $t_1 = 1.0$  and consider two different values of  $t_0$  to represent the two distinct phases:  $t_0 = 0.5$  for topological phase with winding number equals to one and  $t_0 = 1.5$  for the trivial phase.

### 2. 1D Kitaev chain [14] (Chern-Simons $Z_2$ )

$$H_0(k) = (-2t \cos k - \mu) \sigma_z + 2\Delta \sin k \sigma_y. \quad (\text{A2})$$

The particle hole operator is  $\sigma_x K$ . The product of all the unused Dirac matrices is  $W = \sigma_x$ . This model Hamiltonian falls into the symmetry class D with a  $Z_2$  classification, the associated topological invariant is called Chern-Simons  $Z_2$  [8]. We fix  $t = 1, \Delta = 0.5$  and use two different values of  $\mu$  to represent the two distinct phases:  $\mu = 1.0$  for topological phase and  $\mu = 3.0$  for the trivial phase.

### 3. 2D Chern Insulator (The Chern number)

$$H_0(\mathbf{k}) = (M + 4B - 2B \cos k_x - 2B \cos k_y) \sigma_z + 2A \sin k_x \sigma_x + 2A \sin k_y \sigma_y. \quad (\text{A3})$$

The Particle hole operator is  $\sigma_x K$ . The product of all the unused Dirac matrices is  $W = \sigma_0$ . This model Hamiltonian falls into the symmetry class D

with a  $Z$  classification, the associated topological invariant is called Chern number [8, 9, 11, 12]. We fix  $A = 1, B = 1$  and consider two different values of  $M$  to represent the two distinct phases:  $M = -2$  for topological phase with Chern number equals to one and  $M = 2$  for the trivial phase.

#### 4. 2D BHZ model [18, 19]( Fu-Kane $Z_2$ )

$$H_0(k) = 2\Delta \sin k_x s_x \otimes \sigma_z + 2\Delta \sin k_y s_y \otimes \sigma_0 + \{2t(\cos k_x + \cos k_y) - \mu\} s_z \otimes \sigma_0. \quad (\text{A4})$$

The Time reversal operator is  $s_0 \otimes (-i\sigma_y)K$ , Particle hole operator is  $s_x \otimes \sigma_0K$ , and the chiral operator is  $s_x \otimes \sigma_y$ . The product of all the unused Dirac matrices is  $W = is_0 \otimes \sigma_z$ . This model Hamiltonian falls into the symmetry class DIII with a  $Z_2$  classification, the associated topological invariant is called Fu-Kane  $Z_2$  invariant in literature[8, 15–19]. We fix  $t = -1, \Delta = 0.5$  and use two different values of  $\mu$  to represent the two distinct phases:  $\mu = -3.0$  for topological phase and  $\mu = -5.0$  for the trivial

phase.

#### Appendix B: REDUCED FORM OF OUR REGULARIZED UNIVERSAL TOPOLOGICAL LOCAL MARKERS

In this part, we show our regularized universal topological local markers can be reduced to the local markers proposed in [44] in the thermodynamic limit. Firstly, the commutator  $[\hat{x}_i, H]$  is bounded regardless of the lattice size for local Hamiltonian with a finite gap [28, 29, 47], in the thermodynamic limit, the relevant part is only the leading term

$$\frac{1}{2}(X_i H X_i^\dagger - X_i^\dagger H X_i) \sim -i \frac{2\pi}{L_i} [\hat{x}_i, H]. \quad (\text{B1})$$

on the other hand

$$H[\hat{x}_i, H] = -2(Q\hat{x}_i P + P\hat{x}_i Q), \quad (\text{B2})$$

Then, our universal topological operator is reduced to (we have used  $H^2 = 1$ )

$$C = N_D(I_N \otimes W)(Q\hat{x}_1 P + P\hat{x}_1 Q)(Q - P)(Q\hat{x}_2 P + P\hat{x}_2 Q) \cdots (Q - P)(Q\hat{x}_i P + P\hat{x}_i Q) \cdots (Q - P)(Q\hat{x}_D P + P\hat{x}_D Q) \quad (\text{B3})$$

with  $N_D = i^D 2^{2D} \pi^D / 2^s c V_D$ . By considering  $QP = PQ = 0$ , only two terms survive in equation (B3), which are precisely the alternating order terms between  $P$  and  $Q$ , namely,

$$C = N_D(I_N \otimes W)[Q\hat{x}_1 P\hat{x}_2 Q \cdots \hat{x}_D O + (-1)^{D-1} P\hat{x}_1 Q\hat{x}_2 P \cdots \hat{x}_D \bar{O}], \quad (\text{B4})$$

where we have absorbed a possible minus sign into the coefficient  $c$  in  $N_D$ , and  $\{O, \bar{O}\} = \{Q, P\}$  for the even  $D$  case and  $\{O, \bar{O}\} = \{P, Q\}$  for the odd  $D$  case owing to the alternating ordering of the projectors  $Q$  and  $P$ . Equation (B4) is just the topological operator defined in [44].

- 
- [1] A. Altland and M. R. Zirnbauer, Nonstandard symmetry classes in mesoscopic normal-superconducting hybrid structures, *Physical Review B* **55**, 1142 (1997).
- [2] A. P. Schnyder, S. Ryu, A. Furusaki, and A. W. W. Ludwig, Classification of topological insulators and superconductors in three spatial dimensions, *Physical Review B* **78**, 195125 (2008).
- [3] A. P. Schnyder, S. Ryu, A. Furusaki, and A. W. W. Ludwig, Classification of Topological Insulators and Superconductors, in *AIP Conference Proceedings* (2009) pp. 10–21, arXiv:0905.2029 [cond-mat].
- [4] A. Kitaev, Periodic table for topological insulators and superconductors, in *AIP Conference Proceedings*, Vol. 1134 (American Institute of Physics, 2009) pp. 22–30.
- [5] S. Ryu, A. P. Schnyder, A. Furusaki, and A. W. Ludwig, Topological insulators and superconductors: Tenfold way and dimensional hierarchy, *New Journal of Physics* **12**, 065010 (2010).
- [6] M. Z. Hasan and C. L. Kane, *Colloquium* : Topological insulators, *Reviews of Modern Physics* **82**, 3045 (2010).
- [7] X.-L. Qi and S.-C. Zhang, Topological insulators and superconductors, *Reviews of Modern Physics* **83**, 1057 (2011).
- [8] C.-K. Chiu, J. C. Teo, A. P. Schnyder, and S. Ryu, Classification of topological quantum matter with symmetries, *Reviews of Modern Physics* **88**, 035005 (2016).
- [9] K. v. Klitzing, G. Dorda, and M. Pepper, New method for high-accuracy determination of the fine-structure constant based on quantized hall resistance, *Physical Review Letters* **45**, 494 (1980).
- [10] R. B. Laughlin, Quantized Hall conductivity in two dimensions, *Physical Review B* **23**, 5632 (1981).
- [11] D. J. Thouless, M. Kohmoto, M. P. Nightingale, and M. den Nijs, Quantized Hall conductance in a two-dimensional periodic potential, *Physical review letters* **49**, 405 (1982).
- [12] F. D. M. Haldane, Model for a quantum Hall effect without Landau levels: Condensed-matter realization of the

- parity anomaly, *Physical review letters* **61**, 2015 (1988).
- [13] W. P. Su, J. R. Schrieffer, and A. J. Heeger, Soliton excitations in polyacetylene, *Physical Review B* **22**, 2099 (1980).
- [14] A. Y. Kitaev, Unpaired Majorana fermions in quantum wires, *Physics-Uspekhi* **44**, 131 (2001).
- [15] C. L. Kane and E. J. Mele, Quantum spin Hall effect in graphene, *Physical review letters* **95**, 226801 (2005).
- [16] C. L. Kane and E. J. Mele,  $Z_2$  topological order and the quantum spin Hall effect, *Physical review letters* **95**, 146802 (2005).
- [17] L. Fu and C. L. Kane, Time reversal polarization and a  $Z_2$  adiabatic spin pump, *Physical Review B* **74**, 195312 (2006).
- [18] B. A. Bernevig, T. L. Hughes, and S.-C. Zhang, Quantum spin Hall effect and topological phase transition in HgTe quantum wells, *science* **314**, 1757 (2006).
- [19] B. A. Bernevig and S.-C. Zhang, Quantum spin hall effect, *Physical Review Letters* **96**, 106802 (2006).
- [20] J. Bellissard, A. van Elst, and H. Schulz-Baldes, The non-commutative geometry of the quantum Hall effect, *Journal of Mathematical Physics* **35**, 5373 (1994).
- [21] E. Prodan, Non-commutative tools for topological insulators, *New Journal of Physics* **12**, 065003 (2010).
- [22] E. Prodan, T. L. Hughes, and B. A. Bernevig, Entanglement Spectrum of a Disordered Topological Chern Insulator, *Physical Review Letters* **105**, 115501 (2010).
- [23] E. Prodan, Disordered topological insulators: A non-commutative geometry perspective, *Journal of Physics A: Mathematical and Theoretical* **44**, 113001 (2011).
- [24] Y. Xue and E. Prodan, Noncommutative Kubo formula: Applications to transport in disordered topological insulators with and without magnetic fields, *Physical Review B* **86**, 155445 (2012).
- [25] C. Bourne and E. Prodan, Non-commutative Chern numbers for generic aperiodic discrete systems, *Journal of Physics A: Mathematical and Theoretical* **51**, 235202 (2018).
- [26] E. Prodan, B. Leung, and J. Bellissard, The non-commutative  $n$ -th chern number ( $n \geq 1$ ), *Journal of Physics A: Mathematical and Theoretical* **46**, 485202 (2013).
- [27] R. Exel and T. A. Loring, Invariants of almost commuting unitaries, *Journal of Functional Analysis* **95**, 364 (1991).
- [28] M. B. Hastings and T. A. Loring, Almost commuting matrices, localized Wannier functions, and the quantum Hall effect, *Journal of mathematical physics* **51** (2010).
- [29] M. B. Hastings and T. A. Loring, Topological insulators and C\*-algebras: Theory and numerical practice, *Annals of Physics* **326**, 1699 (2011).
- [30] T. A. Loring and M. B. Hastings, Disordered topological insulators via C\*-algebras, *EPL (Europhysics Letters)* **92**, 67004 (2011).
- [31] I. Mondragon-Shem, T. L. Hughes, J. Song, and E. Prodan, Topological criticality in the chiral-symmetric AIII class at strong disorder, *Physical review letters* **113**, 046802 (2014).
- [32] L. Lin, Y. Ke, and C. Lee, Real-space representation of the winding number for a one-dimensional chiral-symmetric topological insulator, *Physical Review B* **103**, 224208 (2021).
- [33] R. Bianco and R. Resta, Mapping topological order in coordinate space, *Physical Review B* **84**, 241106 (2011).
- [34] U. Gebert, B. Irsigler, and W. Hofstetter, Local Chern marker of smoothly confined Hofstadter fermions, *Physical Review A* **101**, 063606 (2020).
- [35] P. d'Ornellas, R. Barnett, and D. K. K. Lee, Quantized bulk conductivity as a local Chern marker, *Physical Review B* **106**, 155124 (2022).
- [36] J. D. Hannukainen, M. F. Martínez, J. H. Bardarson, and T. K. Kvorning, Local Topological Markers in Odd Spatial Dimensions and Their Application to Amorphous Topological Matter, *Physical Review Letters* **129**, 277601 (2022).
- [37] M. S. M. De Sousa, A. L. Cruz, and W. Chen, Mapping quantum geometry and quantum phase transitions to real space by a fidelity marker, *Physical Review B* **107**, 205133 (2023).
- [38] P. B. Melo, S. A. S. Júnior, W. Chen, R. Mondaini, and T. Paiva, Topological marker approach to an interacting Su-Schrieffer-Heeger model, *Physical Review B* **108**, 195151 (2023).
- [39] P. Molignini, B. Lapierre, R. Chitra, and W. Chen, Probing Chern number by opacity and topological phase transition by a nonlocal Chern marker, *SciPost Physics Core* **6**, 059 (2023).
- [40] N. Baù and A. Marrazzo, Local Chern marker for periodic systems, *Physical Review B* **109**, 014206 (2024).
- [41] N. Baù and A. Marrazzo, Theory of local  $Z_2$  topological markers for finite and periodic two-dimensional systems, *Physical Review B* **110**, 054203 (2024).
- [42] A. Cerjan, T. A. Loring, and H. Schulz-Baldes, Local Markers for Crystalline Topology, *Physical Review Letters* **132**, 073803 (2024).
- [43] G. Von Gersdorff, S. Panahiyan, and W. Chen, Unification of topological invariants in Dirac models, *Physical Review B* **103**, 245146 (2021).
- [44] W. Chen, Universal topological marker, *Physical Review B* **107**, 045111 (2023).
- [45] J. W. Milnor and D. W. Weaver, *Topology from the differentiable viewpoint*, Vol. 21 (Princeton university press, 1997).
- [46] H. Huang and F. Liu, Theory of spin Bott index for quantum spin Hall states in nonperiodic systems, *Physical Review B* **98**, 125130 (2018).
- [47] D. Toniolo, On the Bott index of unitary matrices on a finite torus, *Letters in Mathematical Physics* **112**, 126 (2022).
- [48] D. Toniolo, Time-dependent topological systems: A study of the Bott index, *Physical Review B* **98**, 235425 (2018).
- [49] H. Huang and F. Liu, Quantum spin hall effect and spin bott index in a quasicrystal lattice, *Physical Review Letters* **121**, 126401 (2018).
- [50] J. Song and E. Prodan, AIII and BDI topological systems at strong disorder, *Physical Review B* **89**, 224203 (2014).
- [51] J. Li, R.-L. Chu, J. K. Jain, and S.-Q. Shen, Topological anderson insulator, *Physical review letters* **102**, 136806 (2009).
- [52] C.-A. Li, B. Fu, Z.-A. Hu, J. Li, and S.-Q. Shen, Topological phase transitions in disordered electric quadrupole insulators, *Phys. Rev. Lett.* **125**, 166801 (2020).